Available online at www.sciencedirect.com
ScienceDirect
Earth and Planetary Science Letters 261 (2007) 635–648
EPSL
www.elsevier.com/locate/epsl

Noble gas compositions of the lithospheric mantle below the Chyulu Hills volcanic field, Kenya

Jens Hopp *, Mario Trieloff, Rainer Altherr

Mineralogisches Institut, Universität Heidelberg, Im Neuenheimer Feld 236, D-69120 Heidelberg, Germany

Received 9 March 2007; received in revised form 17 July 2007; accepted 17 July 2007
Available online 24 July 2007
Editor: R.W. Carlson

Abstract

We performed a noble gas isotope study on mantle xenoliths from the Quaternary volcanic field of Chyulu Hills, S Kenya, c. 100 km east of the Kenya rift graben. $^{4}He/^{3}He$ ratios were in the range of 100 000–120 000 and indistinguishable from other subcontinental lithospheric mantle compositions worldwide and similar to most results of the East African rift system. $^{21}Ne/^{22}Ne$ ratios corrected for atmospheric contributions displayed less nucleogenic values compared to mid ocean ridge basalts. This requires addition of Ne from a more primitive mantle source, that could be assigned to the postulated Kenyan mantle 'plume' or alternatively might be attributed to the 'high $^{3}He/^{4}He$' Afar hotspot c. 2000 km distant. Whereas He and Ne isotopes reflect a rather homogeneous source composition, we observe a variable air corrected Ar isotopic composition. This might mirror additional contributions of atmospheric fluids strongly enriched in Ar. Nevertheless, in the least contaminated xenolith we were able to calculate a maximum $^{40}Ar/^{36}Ar$ ratio of 34,800±500 assuming a mantle $^{20}Ne/^{22}Ne = 12.5$. This is regarded as best approximation of the real $^{40}Ar/^{36}Ar$ ratio of the investigated mantle source. The same sample showed the highest observed $^{129}Xe/^{130}Xe$ and $^{136}Xe/^{130}Xe$ ratios of 7.01±0.12 and 2.37±0.05, respectively. The correlation of $^{129}Xe/^{130}Xe$–$^{136}Xe/^{130}Xe$ ratios is in broad agreement with mantle Xe in OIB and MORB sources. Within uncertainties a minor contribution of crustally derived xenon is possible, though not compelling.

Keywords: noble gas isotopes; subcontinental lithosphere; Kenya rift; mantle plume

1. Introduction

The Kenya Rift is part of the East African Rift (EAR) system that is the largest currently active continental rift system on Earth and presumably represents the early stages of continental disintegration (Fig. 1). The first magmatism in the Kenyan Rift branch started in late Oligocene in N Kenya (McDougall and Watkins, 1988), approximately contemporaneously to the extrusion of the Ethiopian Flood basalts c. 30 Ma ago (Ukstins et al., 2002). Rifting and lithospheric thinning progressively propagated south- and eastward (Baker, 1987; Morley, 1999). The Kenya Rift graben roughly follows the contact between the margin of the Tanzanian craton and the Neoproterozoic Pan-African crust (Fig. 1), which is probably related to ancient shear zones associated with the Pan-African fold belt.

Today, extension rates seem to be too small for creating the voluminous magmatism in the Kenya area by

* Corresponding author. Tel.: +49 6221 544895; fax: +49 6221 544805.
E-mail address: jhopp@min.uni-heidelberg.de (J. Hopp).

0012-821X/$ - see front matter © 2007 Elsevier B.V. All rights reserved.
doi:10.1016/j.epsl.2007.07.027

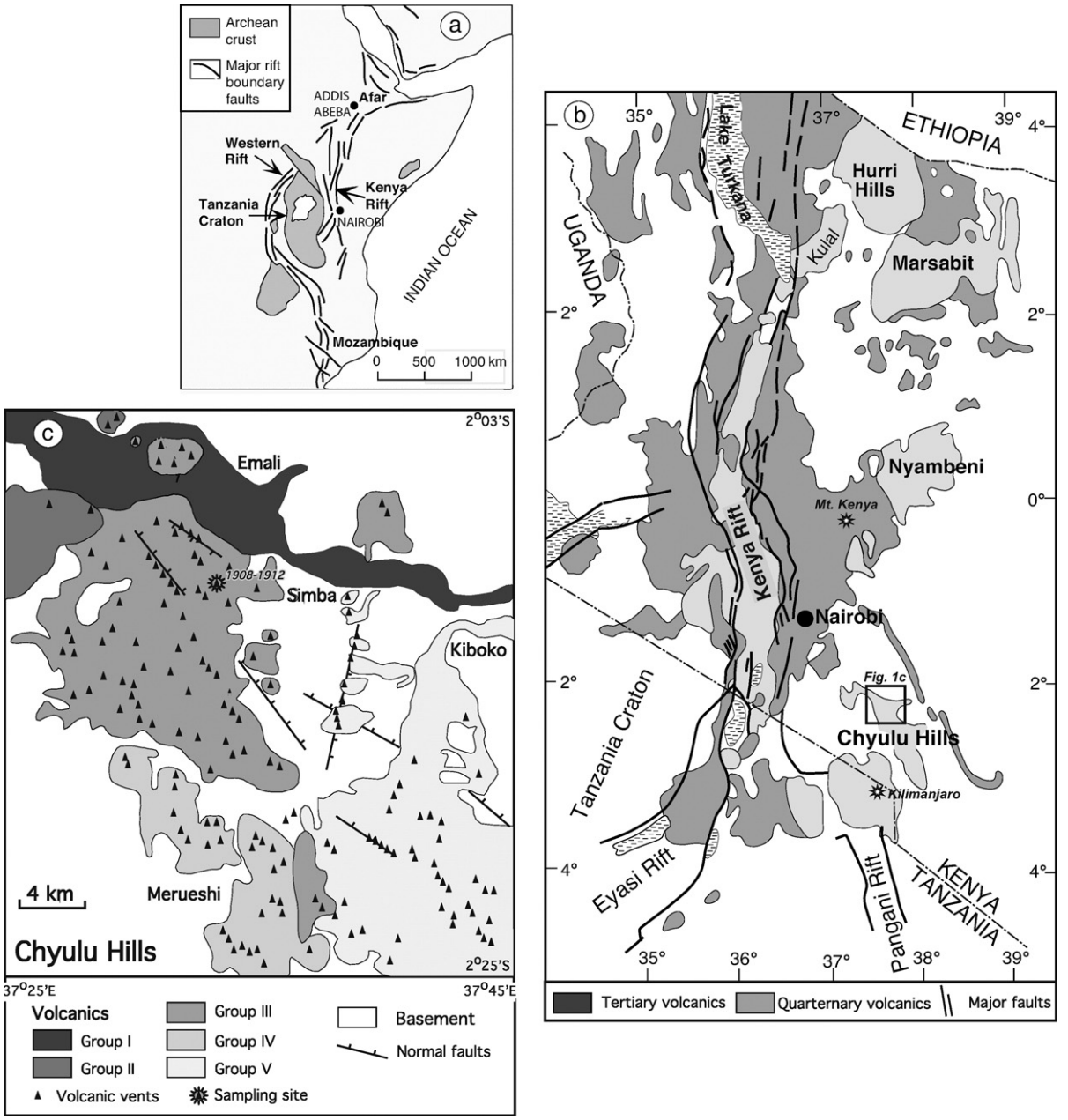

Fig. 1. a) Map of the East African Rift system. b) Distribution of Tertiary and Quaternary volcanic fields in Kenya, Chyulu Hills in southern part. c) Geologic map of part of Chyulu Hills and sampling site. Group 1 and 2: SiO_2-undersaturated foidites; groups 3 and 4: basanites; group 5: alkali basalts.

simple decompression melting (Ebinger et al., 1989). In addition, Kenya forms a topographic high, the East African Plateau. Seismic studies showed that there is a steep-sided low velocity zone present beneath the Kenya Rift (Nyblade et al., 2000; Sebai et al., 2006; Weeraratne et al., 2003). This might indicate upwelling of hot, less dense mantle material in a thermal 'plume', that conductively supplies the necessary heat for extensive mantle melting. It was suggested that this anomaly is coupled with the impact of a major 'plume' head at the Afar triangle in Ethiopia (Ebinger and Sleep, 1998), where seismological data indicate a broad mantle region of low p-wave velocity (Benoit et al., 2006; Debayle et al., 2001). However, it remains to be resolved inhowfar seismic observations of deeper mantle sections can be associated with current magmatism at the EAR system.

Several studies on Sr–Nd–Pb isotope systematics and trace element characteristics of mantle derived samples from the East African Rift system (carbonatites, xenoliths, basalts etc.) had been performed to deconvolve the geochemical fingerprints of possible mantle sources and by which processes they interact. Most studies revealed locally defined correlations in Sr–Nd and Pb–Pb isotope space, but on a regional scale correlations are less clear (e.g. Bell and Tilton, 2001; Furman and Graham, 1999; Furman et al., 2006; Kalt et al., 1997; Macdonald et al., 2001; Pik et al., 1999; Rogers et al., 2000, 2006; Späth et al., 2001). Empirically, endmember compositions are ascribed as HIMU and EM1-type, in analogy to well-known oceanic signatures (Zindler and Hart, 1986). In addition, some authors defined distinct compositions representing the Kenyan and Afar mantle 'plume' source (Rogers et al., 2000). However, linking isotope compositions with source regions still remains model dependent. Consequently, the influence of the local (Pan-African or cratonic) lithosphere on magma compositions in contrast to deep mantle 'plume' contributions still remains a matter of debate.

In contrast to the more ambiguous isotope systems of Sr–Nd–Pb noble gas isotopes, in particular of He and Ne, are widely used to characterize a possible 'plume' component in igneous rocks. The mantle source of hotspots like Loihi (Hiyagon et al., 1992; Honda et al., 1991; Trieloff et al., 2000; Valbracht et al., 1997), Iceland (Hilton et al., 1998; Moreira et al., 2001; Trieloff et al., 2000; Stuart et al., 2003) and others is relatively enriched in primordial noble gas isotopes in comparison with the asthenospheric source of mid ocean ridge basalts (MORB) (Marty, 1989; Moreira et al., 1998; Sarda et al., 1988) and the subcontinental lithospheric mantle (Dunai and Porcelli, 2002; Gautheron and Moreira, 2002). Importantly, $^{3}He/^{4}He$ ratios observed at Afar c. 2000 km north of the Chyulu Hills volcanic field reach up to 20 R_A (Marty et al., 1996; Pik et al., 2006; Scarsi and Craig, 1996) (atmospheric ratio 1 $R_A = 1.384 \cdot 10^{-6}$, Clarke et al., 1969), significantly higher than elsewhere in Africa (Pik et al., 2006). Most He data obtained on worldwide samples of the subcontinental lithospheric mantle (SCLM) including Kenya showed a rather restricted range in $^{3}He/^{4}He$ ratios (Buikin et al., 2005; Darling et al., 1995; Day et al., 2005; Hopp et al., 2004; Matsumoto et al., 1998, 2000; Pik et al., 2006) that are slightly more radiogenic than most MORB samples, and thus not indicative for a Loihi-type 'plume' source. In contrary, at several locations worldwide the associated Ne isotopes pointed to the involvement of a significant amount of 'plume' Ne with less nucleogenic (air corrected) mantle $^{21}Ne/^{22}Ne$ ratios than MORB (Barfod et al., 1999; Buikin et al., 2005; Hopp et al., 2004; Matsumoto et al., 1997). In particular contributions of 'plume' neon were observed in ultramafic rocks (Hopp et al., 2004) and basalts (Moreira et al., 1996) from the Red Sea region >2000 km distant from its proposed mantle source origin at the Afar triangle. Hence, the Ne isotope system seems more suited for the investigation of contributions from a more primitive mantle source in continental lithospheric environments.

Here we report the results of a noble gas study on mantle xenoliths of the Chyulu Hills volcanic field in southern Kenya (Fig. 1b), which had been subject of extensive petrologic, petrographic, geochemical and seismic work in the past (Altherr et al., in revision; Henjes-Kunst and Altherr, 1992; Novak et al., 1997; Späth et al., 2001).

2. Geology/samples

The Chyulu Hills volcanic field is located in Southern Kenya about 100 km east of the Kenyan Rift branch (Fig. 1b). It mainly consists of Quaternary nephelinites, basanites and alkali basalts (Fig. 1) (Haug and Strecker, 1995; Späth et al., 2001). All xenoliths investigated in this study had been collected from one basanitic volcanic vent (Fig.1c, group 3 basanites according to Haug and Strecker, 1995). An extensive petrographic and petrologic study on a large suite of mantle xenoliths revealed a local lithospheric thickness of about 115 km (Altherr et al., in revision; Henjes-Kunst and Altherr, 1992). The lowest part of this subcontinental lithospheric mantle (SCLM) consists of fertile garnet lherzolites and depleted porphyroclastic spinel harzburgites. There is no information about the 105–80 km depth range. At 80–60 km depleted harzburgite and (olivine) websterite are the most abundant rock types whereas the top layer of the mantle section (60–40 km) comprises mainly orthopyroxenite, websterite and very depleted granular harzburgite. The results of geothermobarometry indicates a slow cooling of the mantle portion above 80 km, probably having started at the time of stabilization of the lithospheric mantle during or after the Pan-African orogenic event (c. 550–500 Ma ago) (Altherr et al., in revision; Ulianov et al., 2006). There is neither petrologic nor seismic evidence for a Tertiary to recent regional thermal disturbance of the SCLM below the Chyulu Hills. Instead, present heat input seems restricted to small volumes of shallow magma intrusives whose mantle source still remains unclear (Altherr et al., in revision).

In this study, we analysed handpicked orthopyroxene separates of a spinel lherzolite (Ke 1911/4), two garnet orthopyroxenites (Ke 1910/11a and Ke 1911/15), and two spinel harzburgites (Ke 1911/3 and Ke 1911/6).

Table 1
He, Ne and Ar isotopic composition of mantle xenoliths from the Chyulu Hills, Kenya

Extraction[a]	^{4}He (10^{-7})[b]	^{4}He/^{3}He	^{3}He/^{4}He (in R_A)[c]	^{22}Ne (10^{-12})[b]	^{20}Ne/^{22}Ne	^{21}Ne/^{22}Ne	^{36}Ar (10^{-11})[b]	^{40}Ar/^{36}Ar
Ke 1910/11a opx (garnet orthopyroxenite) 5.6280 g								
150×	2.27 (7)	106 760 (3080)	6.77 (20)	6.37 (3)	10.42 (4)	0.0348 (4)	17.8 (6)	3870 (50)
500×	2.43 (7)	109 650 (3170)	6.59 (19)	5.49 (3)	10.71 (5)	0.0374 (5)	13.5 (5)	5950 (70)
1200×	2.89 (9)	109 230 (3170)	6.61 (19)	5.51 (2)	10.94 (5)	0.0392 (5)	12.8 (5)	7830 (100)
2700×	2.05 (6)	108 290 (3190)	6.67 (20)	3.52 (2)	11.25 (6)	0.0435 (6)	7.3 (3)	10 880 (140)
5200×	1.10 (3)	111 660 (3430)	6.47 (20)	1.83 (1)	11.52 (8)	0.0456 (10)	3.4 (3)	14 380 (230)
Ke 1911/3 opx (spinel harzburgite) 4.6609 g								
200×	1.21 (12)	106 460 (2090)	6.79 (13)	7.49 (2)	10.30 (3)	0.0340 (3)	16.9 (11)	2110 (80)
700×	1.19 (12)	113 470 (2340)	6.37 (13)	4.69 (2)	10.74 (4)	0.0375 (5)	9.0 (6)	4060 (150)
2000×	1.42 (14)	110 090 (1750)	6.56 (10)	4.61 (2)	11.31 (5)	0.0415 (5)	7.7 (6)	6360 (240)
4500×	0.63 (6)	109 180 (2500)	6.62 (15)	1.89 (1)	11.72 (8)	0.0439 (9)	3.1 (2)	8770 (320)
Ke 1911/4 opx (spinel lherzolite) 5.0981 g								
150×	2.79 (19)	128 490 (2020)	5.62 (9)	25.49 (5)	10.04 (2)	0.0310 (2)	63.9 (23)	1170 (10)
600×	3.50 (24)	118 000 (1840)	6.12 (10)	17.77 (4)	10.29 (2)	0.0327 (3)	44.7 (16)	2040 (50)
1600×	2.29 (15)	120 010 (2000)	6.02 (10)	7.21 (3)	10.68 (5)	0.0369 (4)	17.1 (6)	3800 (40)
4100×	1.05 (7)	123 280 (2720)	5.86 (13)	2.58 (1)	11.08 (5)	0.0412 (7)	6.0 (2)	6150 (50)
Ke 1911/6 opx (spinel harzburgite) 4.9376 g								
200×	0.89 (9)	114 040 (2410)	6.34 (13)	2.07 (1)	10.16 (6)	0.0337 (6)	5.31 (42)	1900 (80)
700×	1.00 (10)	111 780 (2290)	6.46 (13)	1.66 (1)	10.41 (8)	0.0348 (9)	4.59 (29)	2530 (90)
3000×	1.12 (11)	113 990 (2410)	6.34 (13)	1.38 (1)	10.67 (9)	0.0359 (10)	4.41 (28)	3760 (140)
Ke 1911/15 opx (garnet orthopyroxenite) 5.5665 g								
200×	0.38 (2)	95 160 (1760)	7.59 (16)	1.43 (1)	11.03 (10)	0.0404 (8)	4.76 (8)	5270 (50)
700×	0.38 (2)	100 280 (2580)	7.21 (20)	1.11 (1)	11.40 (13)	0.0450 (11)	3.31 (3)	8280 (100)
3000×	0.43 (2)	102 950 (1920)	7.02 (15)	1.32 (1)	11.67 (13)	0.0477 (11)	3.78 (3)	9180 (90)
Air		722 543	≡1		9.8	0.029		296

Numbers in parentheses refer to the last digits and are 1σ-uncertainties.
[a] Cumulative number of strokes.
[b] Concentrations in cm^3 STP/g.
[c] 1 R_A = Atmospheric ratio of ^{3}He/^{4}He = $1.384 \cdot 10^{-6}$ (Clarke et al., 1969).

Garnet is mostly replaced by a symplectite. In Ke 1911/4 dolomite aggregates enclosed in silicate glass had been found. The sampled *P–T* range encompasses 1.8–2.4 GPa and 950–1040 °C, respectively (Altherr et al., in revision).

3. Experimental methods

Noble gas analyses were performed at the Max Planck Institute for nuclear physics, Heidelberg, with a mass spectrometer of type VG 3600. Sample gas was released by stepwise crushing in three ball mills. Hot and cold Ti-sponge and Zr–Al getters were used for purification of the extracted gas. Ar and Xe were first trapped at a charcoal cooled with liquid nitrogen and thus separated from He and Ne. The latter were trapped at a charcoal hold at 11 K. Subsequently, separation of He and Ne was achieved at 30 K, and Ne was released at 60 K to avoid any residual Ar contributions. We separated Ar and Xe from the charcoal at −50 °C and expanded the Ar in the glass line. For measurement, only known partial volumes of Ar had been used. The Xe still contained about 7% of Ar during analyses. Kr had been not measured. The spectrometer background was monitored before introduction of the sample gases. The ion current of ^{4}He, ^{40}Ar and ^{36}Ar were measured directly with a Faraday cup. The other isotopes and ^{36}Ar had been analysed in ion counting mode. The signal ratio between analog and digital measurement was determined frequently. In the case of Ne, we also routinely detected the masses 18, 40, 42 and 44 and corrected for mass interferences on neon isotopes. However, these corrections never exceeded 0.1%. Correction for instrumental mass fractionation was achieved by measurement of standard gases with air composition (Ne, Ar, Xe). For He a spiked standard gas (Potsdam standard) with ^{3}He/^{4}He of 14.7 R_A was used. System blanks had been in the range

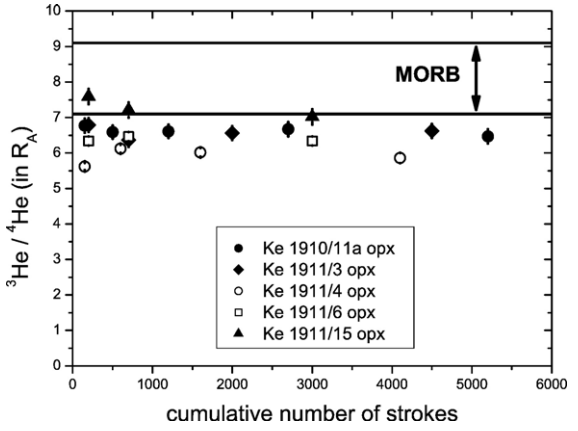

Fig. 2. ^{3}He/^{4}He ratios normalized to atmospheric value of $1.384 \cdot 10^{-6}$ (Clarke et al., 1969) plotted versus cumulative number of strokes. Uncertainties are 1σ.

of 7–$8.5 \cdot 10^{-9}$ cm^3 STP ^{4}He; 1.9–$5.8 \cdot 10^{-12}$ cm^3 STP ^{20}Ne; 0.9–$3.1 \cdot 10^{-12}$ cm^3 STP ^{36}Ar; 4.9–$17.7 \cdot 10^{-15}$ cm^3 STP ^{132}Xe. Within uncertainties, measured blanks had been indistinguishable to isotopic composition of air.

Given uncertainties include errors of standard measurements, and interference/blank corrections (20% uncertainty in absolute blank). Uncertainties of absolute concentrations of the standard gases are 10%, however, elemental ratios between Ne, Ar and Xe base on air compositions and are estimated to have an uncertainty of about 5% (mainly due to volume corrections).

4. Results

4.1. Helium

^{3}He/^{4}He ratios are in the range of 5.6–7.6 R_A, dominantly between 6 and 7 R_A (Table 1, Fig. 2), and thus slightly more radiogenic in comparison to most MORB samples. Within uncertainties, no significant intrasample variations were observed, i.e. no contribution of in situ radiogenic ^{4}He or cosmogenic/nucleogenic ^{3}He were detectable. These results are in full agreement with previous studies on East African mantle rocks (Pik et al., 2006) or Kenyan well gases (Darling et al., 1995) and similar to global ^{3}He/^{4}He isotope systematics of subcontinental mantle lithosphere (e.g. Dunai and Porcelli, 2002; Gautheron and Moreira, 2002).

4.2. Neon

In a neon three isotope diagram (Fig. 3) all data follow a rather narrow and well defined mixing trend between air and a mantle endmember composition, pointing to a rather homogeneous neon isotope composition. Knowledge of the respective mantle ^{20}Ne/^{22}Ne value then allows calculation of an air corrected mantle ^{21}Ne/^{22}Ne ratio. Basing on the improved database of the last years (Ballentine et al., 2005; Holland and Ballentine, 2006; Hopp and Trieloff, 2005; Trieloff et al., 2000; 2002) a mantle ^{20}Ne/^{22}Ne ratio of 12.5 appears most likely and has been interpreted to correspond to a meteoritic implanted solar wind component (Ballentine et al., 2005; Trieloff et al., 2000). This contrasts with previous views of an ubiquitous (unfractionated) solar wind-type mantle ^{20}Ne/^{22}Ne composition of c. 13.8 (e.g. Honda et al., 1991), for which however, direct evidence is ambiguous. So far a uniform mantle ^{20}Ne/^{22}Ne composition valid for all mantle reservoirs is not proven yet. However, an unfractionated solar wind mantle ^{20}Ne/^{22}Ne composition of 13.8 is estimated to encompass only small heterogeneities within Earth's mantle (Ballentine et al., 2005) and appears – if at all – of minor importance. Consequently we use a mantle ^{20}Ne/^{22}Ne of 12.5 for extrapolation to a mantle ^{21}Ne/^{22}Ne value. With the assumption of one homogeneous mantle neon isotopic composition documented in every individual sample, we calculated sample specific mantle ^{21}Ne/^{22}Ne ratios (Table 2) from all extractions of one xenolith by linear regression analysis. Our results agree with a less nucleogenic lithospheric mantle source compared to MORB data

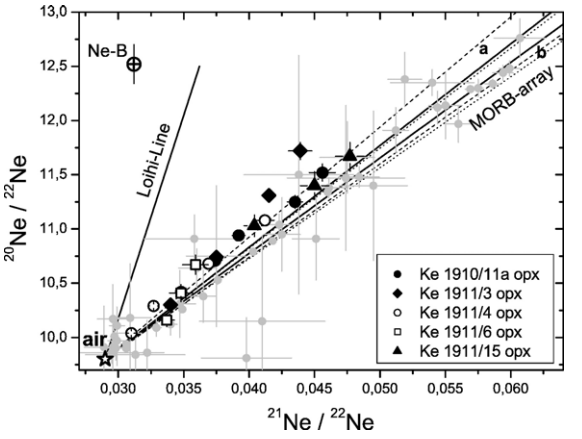

Fig. 3. Neon three-isotope diagram. Solid lines indicate mixing trends between an atmospheric, and a Loihi-type and MORB-component, respectively. Two lines are shown for different reported MORB glass suites grey symbols: Trend a) from Niedermann and Bach (1998) (dashed 2σ-confidence bands). Trend b) from Sarda et al. (1988) (dotted 2σ-confidence bands). High precision data of Moreira et al. (1998) plot along trend b). Apparently, the Kenyan data are significantly plotting to the left of all MORB arrays, but mantle ^{21}Ne/^{22}Ne compositions are significantly more nucleogenic than a Loihi-type mantle source composition. Sample specific mantle ^{21}Ne/^{22}Ne ratios had been calculated by linear regression and are given in Table 2. Uncertainties are 1σ.

Table 2
Summary of results from regression analysis

Sample	$^{21}Ne/^{22}Ne_{12.5}$	$^{40}Ar/^{36}Ar_{12.5}$
Ke 1910/11a opx	0.0546±0.0013	34 811±914
Ke 1911/3 opx	0.0522±0.0012	13 333±816
Ke 1911/4 opx	0.0511±0.0018	20 730±480
Ke 1911/6 opx	0.0554±0.0047	8203±632
Ke 1911/15 opx	0.0554±0.0028	17 492±368
MORB (S88)	0.0596±0.0004	–
MORB (M98)	0.0597±0.0002	–
MORB (NB98)	0.0578±0.0012	–
Sample	$^{36}Ar/^{22}Ne_{9.8}$	$^{36}Ar/^{22}Ne_{12.5}$
Ke 1910/11a opx	32.86+1.75–2.05	10.40+2.59–2.96
Ke 1911/3 opx	23.91±5.57	12.30±5.57
Ke 1911/4 opx	25.68±1.77	20.60±4.20
Ke 1911/6 opx	20.67	54.47
Ke 191115 opx	41.29	22.79
Sample	*r* (Hyp.-Fit)	*r* (Lin.-Fit)
Ke 1910/11a opx	0.385±0.007	0.316±0.092
Ke 1911/3 opx	0.72±0.04	0.51±0.26
Ke 1911/4 opx	0.441±0.007	0.802±0.173
Ke 1911/6 opx	1.53±0.09	2.635
Ke 1911/15 opx	0.50±0.01	0.552

Sample specific $^{21}Ne/^{22}Ne$ and $^{36}Ar/^{22}Ne$ ratios at a mantle $^{20}Ne/^{22}Ne=12.5$ from linear regression with weighted error. Atmospheric $^{36}Ar/^{22}Ne$ ratios are obtained at $^{20}Ne/^{22}Ne=9.8$. Calculated mantle $^{40}Ar/^{36}Ar$ ratios (at $^{20}Ne/^{22}Ne=12.5$) and *r*-curve parameters are from a hyperbolic least square fit assuming a binary mixing trend. For comparison, *r*-values obtained from $^{36}Ar/^{22}Ne$ linear regression results are also listed in last column. M98: Moreira et al. (1998); NB98: Niedermann and Bach (1998); S88: Sarda et al. (1988).

(Fig. 3). To demonstrate this we draw two regression lines and their 95% confidence bands of MORB data in Fig. 3 (Niedermann and Bach, 1998; Sarda et al., 1988) that we had reported previously (Hopp et al., 2004). Only five out of nineteen extraction results fall into the confidence bands defined by the data of Niedermann and Bach (1998), and only one extraction result plot within the confidence bands defined by the data of Sarda et al. (1988). The MORB-line calculated from data of Moreira et al. (1998) is indistinguishable from Sarda et al. (1988), but more precise. For convenience, we listed the extrapolated MORB-values derived from all three studies together with our data in Table 2 (1σ errors).

However, the neon isotope composition of the Kenyan mantle source is still much more nucleogenic compared with primitive sources of some hotspots, e.g. Loihi or Iceland (Honda et al., 1991; Trieloff et al., 2000; Valbracht et al., 1997). In a simple mixing model between a MORB-type ($^{21}Ne/^{22}Ne=0.0595$, Trieloff and Kunz, 2005) and a Loihi-type ($^{21}Ne/^{22}Ne=0.0362$, Trieloff and Kunz, 2005) mantle source composition the neon composition would correspond to a c. 30% contribution of a Loihi-type mantle neon component. A more nucleogenic lithospheric endmember composition ($^{21}Ne/^{22}Ne=0.070$) according to the more radiogenic He composition seems more adequate (Buikin et al., 2005; Hopp et al., 2004), hence the relative proportion of a Loihi-type mantle neon component might even increase to c. 50%. In comparison, the respective amount of a Loihi-type mantle He component would only amount to c. 10% versus 90% of lithospheric He with $^{4}He/^{3}He=120\,000$. All in all our neon results appear to indicate a significant contribution of a primitive 'plume' component in the source region of our investigated xenolith samples.

4.3. Argon

Observed maximum $^{40}Ar/^{36}Ar$ ratios for each sample are 3760 to 14380 (Table 1, Fig. 4). For all xenoliths a correlation with $^{20}Ne/^{22}Ne$ ratios is recognized and interpreted as mixing between an atmospheric and a mantle component with $^{20}Ne/^{22}Ne=9.8$ and 12.5, respectively. However, only for grt–orthopyroxenite Ke 1910/11a and spl–harzburgite Ke 1911/3 a least square fit of the data yielded well defined mixing hyperbolae with low χ^2-values of 0.28 and 0.68, respectively. χ^2-values below 1 indicate, that the data on average agree with the model curve within 1σ-uncertainty (see Buikin et al., 2005 for more details).

In case of spl–harzburgite Ke 1911/6 and spl–lherzolite Ke 1911/4 the regression analysis resulted in a

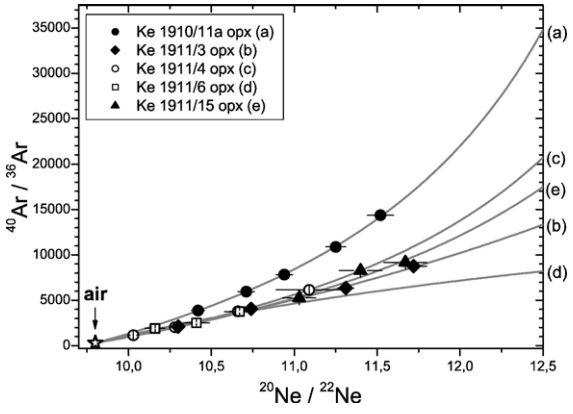

Fig. 4. Diagram showing $^{40}Ar/^{36}Ar$ ratios versus $^{20}Ne/^{22}Ne$ ratios. Sample specific hyperbolic trends are calculated assuming binary mixing between one atmospheric and one mantle endmember, the latter corresponding to a $^{20}Ne/^{22}Ne=12.5$. Letters a–e at righthand-side refer to samples in legend. Results of extrapolations are shown in Table 2. Uncertainties are 1σ.

less well defined mixing trend (χ^2-values of 2.87 and 3.65, respectively) and for grt–orthopyroxenite Ke 1911/15 a mixing curve was only poorly defined, as evidenced by the high χ^2-value of 22. To envisage the range of obtained mixing trajectories we plotted all curves in Fig. 4 together with the data. It is apparent that the extrapolated mantle $^{40}Ar/^{36}Ar$ ratios are variable, ranging from 8000 up to 34 800 (Table 2). This is in contrast with observed rather uniform mantle $^{4}He/^{3}He$ and $^{21}Ne/^{22}Ne$ ratios. Similarly, the curve parameter r_{HYP} (subscript HYP denotes that r values are derived by hyperbolic fit), i.e. the ratio of the mantle and atmospheric $^{36}Ar/^{22}Ne$ ratios varies between 0.39 and 1.53 (Table 2).

To check our fit results, we can independently determine the r values from direct analysis of $^{36}Ar/^{22}Ne$ elemental ratios in a $^{36}Ar/^{22}Ne$ vs $^{20}Ne/^{22}Ne$ isotope space. A simple binary mixture between an atmospheric (defined by $^{20}Ne/^{22}Ne=9.8$) and a mantle component (defined by $^{20}Ne/^{22}Ne=12.5$) should result in a linear trend, which had been calculated via regression analysis for each sample separately (supplementary Fig. 1) and supplies us with respective atmospheric and mantle $^{36}Ar/^{22}Ne$ ratios (Table 2, indices 9.8 and 12.5 indicate the atmospheric and mantle values, respectively). Both, the atmospheric and mantle $^{36}Ar/^{22}Ne$ ratios show intersample variations and in some cases differ significantly from unfractionated air ($^{36}Ar/^{22}Ne=18.7$, Ozima and Podosek, 2002) and an estimated mantle value ($^{36}Ar/^{22}Ne=9.2\pm3.0$, Trieloff et al., 2002; 8.9 ± 0.3, Holland and Ballentine, 2006). Unfortunately the r_{LIN} values (subscript LIN denotes that r values are derived from linear fit) obtained from direct analysis of elemental ratios tend to be less precise. In particular the uncertainties tend to be huge (>100%, not shown in Table 2) for the xenoliths Ke 1911/6 and Ke1911/15 that had been crushed in three steps only. r_{LIN} values of the other three xenoliths agree within 2σ-uncertainty with calculated r_{HYP} parameters (Table 2).

The trapped atmospheric components have $^{36}Ar/^{22}Ne$ ratios higher than unfractionated air, that can be easily explained by the better solubility of Ar compared with Ne in water bearing fluids. The relative solubilities of Ar and Ne in equilibrium with water vary with temperature. At low temperatures (<100 °C) Ar is approximately 2–4 times better soluble as Ne (e.g. Ballentine et al., 2002), i.e. the respective $^{36}Ar/^{22}Ne_{water}$ values are in the range of 40–80. Contact with water, either during exposure at the surface (meteoric waters) or during cleaning in the laboratory, will accordingly result in enhanced atmospheric $^{36}Ar/^{22}Ne$ ratios. The mantle $^{36}Ar/^{22}Ne$ ratio seems also variable. This agrees with results for other locations of sampled subcontinental lithospheric mantle (Eifel, Pannonian Basin, Buikin et al., 2005; Red Sea, Hopp et al., 2007). It appears, that heterogeneous mantle-$^{40}Ar/^{36}Ar$ and mantle-$^{36}Ar/^{22}Ne$ ratios are a widespread phenomenon in rocks of the subcontinental lithospheric mantle. This is further discussed below in Section 5.3.

4.4. Xenon

We found significant contributions of excess ^{129}Xe and $^{131-136}Xe$ relative to ^{130}Xe and atmospheric composition. In a Xe three isotope diagram (Fig. 5) $^{129}Xe/^{130}Xe$ vs $^{136}Xe/^{130}Xe$ the data follow a linear trend with equation $^{129}Xe/^{130}Xe=(2.25\pm0.25)*{}^{136}Xe/^{130}Xe+(1.60\pm0.53)$ (error weighted fit, 1σ uncertainties). The slope is lower than calculated slopes of the common trend observed for MORB (3.125 ± 0.084; Kunz et al., 1998) and Loihi data (2.70 ± 0.16; Trieloff and Kunz, 2005). The nominal deviation from the mantle trend would correspond to an excess fissiogenic ^{136}Xe of c. 25% relative to the total mantle ^{136}Xe. However, within uncertainties our results still agree with previous results on oceanic mantle samples (Fig. 5, MORB, Kunz et al., 1998; Marty, 1989; Staudacher and Allègre, 1982; oceanic islands, Hopp and Trieloff, 2005; Poreda and Farley, 1992; Trieloff et al., 2000, 2002; continental volcanics, Matsumoto et al., 2000; Yokochi and Marty, 2005). Maximum observed $^{129}Xe/^{130}Xe$ and $^{136}Xe/^{130}Xe$ ratios are 7.01 ± 0.12 and 2.37 ± 0.05, respectively (Table 3). These values must be

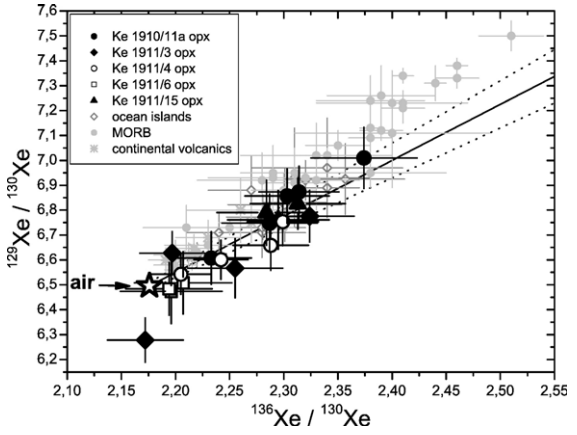

Fig. 5. Xenon three-isotope diagram $^{129}Xe/^{130}Xe$ versus $^{136}Xe/^{130}Xe$. Within uncertainties data follow the mantle mixing trend between atmospheric and mantle derived Xe with characteristic correlated excess in ^{129}Xe and ^{136}Xe. Maximum excess is intermediate compared to maximum values observed in samples from hotspots (Loihi, Iceland, Réunion) and MORB samples. Linear trend displays error weighted fit, dotted lines represent 1σ confidence bands. Error bars are 1σ uncertainties.

Table 3
Xe isotopic composition of mantle xenoliths from the Chyulu Hills, Kenya

Extraction [a]	^{132}Xe (10^{-14}) [b]	^{129}Xe/^{132}Xe	^{130}Xe/^{132}Xe	^{131}Xe/^{132}Xe	^{134}Xe/^{132}Xe	^{136}Xe/^{132}Xe
Ke 1910/11a opx (garnet orthopyroxenite) 5.6280 g						
150×	47.2 (15)	1.007 (8)	0.152 (2)	0.791 (5)	0.397 (3)	0.340 (3)
500×	43.0 (14)	1.018 (7)	0.148 (2)	0.782 (7)	0.396 (3)	0.342 (3)
1200×	46.5 (15)	1.033 (8)	0.150 (2)	0.786 (6)	0.406 (3)	0.348 (3)
2700×	34.1 (11)	1.029 (7)	0.152 (2)	0.787 (5)	0.403 (3)	0.349 (4)
5200×	20.6 (7)	1.031 (9)	0.147 (2)	0.784 (8)	0.401 (5)	0.349 (5)
Ke 1911/3 opx (spinel harzburgite)						
200×	31.1 (18)	0.997 (8)	0.150 (2)	0.790 (5)	0.393 (3)	0.331 (3)
700×	21.6 (12)	0.974 (9)	0.155 (2)	0.777 (8)	0.386 (4)	0.337 (4)
2000×	23.4 (17)	0.989 (6)	0.146 (2)	0.780 (6)	0.386 (4)	0.339 (4)
4500×	12.1 (9)	0.996 (11)	0.152 (2)	0.783 (10)	0.392 (6)	0.342 (4)
Ke 1911/4 opx (spinel lherzolite) 5.0981 g						
150×	64.9 (19)	0.992 (7)	0.152 (2)	0.787 (5)	0.395 (4)	0.334 (2)
600×	59.6 (18)	0.997 (7)	0.151 (1)	0.789 (5)	0.394 (3)	0.339 (2)
1600×	34.6 (10)	1.001 (8)	0.148 (2)	0.786 (5)	0.394 (4)	0.341 (3)
4100×	24.1 (7)	1.003 (8)	0.151 (2)	0.788 (7)	0.398 (4)	0.345 (3)
Ke 1911/6 opx (spinel harzburgite)						
200×	10.3 (7)	1.003 (12)	0.154 (2)	0.793 (10)	0.395 (8)	0.340 (5)
700×	9.8 (7)	0.992 (13)	0.153 (2)	0.792 (9)	0.386 (5)	0.337 (5)
3000×	13.9 (10)	1.000 (10)	0.154 (2)	0.797 (8)	0.384 (6)	0.338 (4)
Ke 1911/15 opx (garnet orthopyroxenite) 5.5665 g						
200×	15.5 (1)	1.008 (7)	0.149 (2)	0.785 (7)	0.396 (5)	0.342 (4)
700×	13.4 (1)	1.032 (11)	0.152 (2)	0.788 (9)	0.415 (5)	0.347 (4)
3000×	16.5 (1)	1.028 (8)	0.151 (2)	0.775 (10)	0.405 (4)	0.348 (5)
Air		0.983	0.151	0.789	0.388	0.329

Numbers in parentheses refer to the last digits and are 1σ-uncertainties.
[a] Cumulative number of strokes.
[b] Concentrations in cm^3 STP/g.

regarded as lower limits, because additional atmospheric contributions might still be present. At highest amount of strokes, observed isotopic compositions of Xe decrease again towards atmospheric composition. This is associated with a relative enrichment of Xe compared with Ne and Ar in course of the crushing process, pointing to an atmospheric Xe contribution with a high Xe/Ar and Xe/Ne ratio compared with unfractionated air values (supplementary Fig. 2 and Fig. 3). The source of this component could be related to a dynamic blank contribution (via frictional heating during crushing) that is hard to quantify. Alternatively, it could reflect a fluid inclusion assemblage preferentially released at higher amounts of strokes with a dominantly fractionated atmospheric composition. This also precludes a determination of a mantle endmember composition with a similar approach as done for ^{40}Ar/^{36}Ar ratios. Apart from these problems we may state that the observed maximum ratio is lower than known MORB ratios and slightly higher than maximum ^{129}Xe/^{130}Xe and ^{136}Xe/^{130}Xe ratios obtained in hotspot derived samples (Fig. 5).

5. Discussion

5.1. Origin of observed noble gas isotope compositions

In the 'Results' section we pointed out that the neon isotopic compositions observed in our xenoliths are in agreement with addition of neon of a Loihi-type mantle 'plume' source. However, other sources or processes may have contributed to the noble gas budget in our xenoliths as well. In the following we first discuss and exclude a significant contribution of in situ radiogenic noble gas isotopes or crustal rare gases. Afterward we consider inhowfar the local lithospheric mantle might be possibly treated as intrinsic mantle component with a unique and distinct less nucleogenic neon isotope composition compared to the asthenospheric mantle source.

5.1.1. In situ radiogenic and crustal contributions

In situ addition of radiogenic (^{4}He*, ^{40}Ar*), nucleogenic (^{21}Ne*) and fissiogenic ($^{131-136}$Xe*) isotopes since time of xenolith emplacement is considered as unlikely, because of the low age of the host volcanics and the lack of potential U-, Th- or K-rich phases in our xenoliths (e.g. apatite, phlogopite, amphibole). Furthermore, application of the crushing technique has proven to considerable discriminate lattice site hosted isotopes derived from radioactive decay reactions (Scarsi, 2000). We could not detect any significant isotope variation in ^{3}He/^{4}He ratios during the crushing process (Fig. 2), that would point to the release of lattice sited radiogenic ^{4}He*. This also excludes a possible cosmogenic origin of some isotopes (^{3}He, ^{21}Ne) possibly produced during surface exposure, which again should be preferentially released at the highest amount of strokes.

Crustal noble gases are another component to be considered. They are highly enriched in radiogenic, nucleogenic and fissiogenic isotopes (e.g. Drescher et al., 1998). For clarity we note, that meteoric waters migrating deep into the crust, but still preserving an atmospheric isotopic composition, do not fall within our definition of crustal noble gases, but would be treated as independent atmospheric component. If crustal noble gases are admixed to a magma before separation of fluids and incorporation into the recovered xenolith, this could certainly change the noble gas isotope compositions within our rocks. So far, the ^{21}Ne/^{22}Ne ratios are less nucleogenic relative to MORB values, and ^{40}Ar/^{36}Ar ratios are in agreement with typical mantle ratios or even lower than expected for a crustal highly radiogenic ^{40}Ar* contribution. The small deviation towards higher ^{136}Xe/^{130}Xe ratios at a given ^{129}Xe/^{130}Xe value compared with oceanic samples could allow a possible c. 25% contribution of fissiogenic ^{136}Xe* to the total (air corrected) ^{136}Xe that could be of crustal origin. However, within the high variance, our Xe data agree with typical mantle compositions (Fig. 5) and cannot be taken as evidence for or against crustal contributions. Eventually, the more radiogenic ^{4}He/^{3}He ratios relative to MORB ratios are frequently found in rocks from the subcontinental lithospheric mantle worldwide (Gautheron and Moreira, 2002; Pik et al., 2006). These rather uniform He compositions would necessitate a similarly uniform contribution of crustal helium during magma transit, independent from crustal age, which is considered as unlikely.

5.1.2. The neon composition of the subcontinental lithospheric mantle source

We may envisage a lithospheric time integrated radiogenic evolution path distinct from the asthenospheric MORB source. With few exceptions, less nucleogenic ^{21}Ne/^{22}Ne ratios compared to MORB ratios seem ubiquitously present in rocks from the subcontinental lithospheric mantle (Buikin et al., 2005; Hopp et al., 2004; Matsumoto et al., 1997). An intrinsic lithospheric component with a less nucleogenic mantle ^{21}Ne/^{22}Ne ratio could be a consequence of a distinct closed system evolution in respect to radiogenic/nucleogenic isotopes. To warrant a higher time integrated ingrowth in radiogenic ^{4}He* and a lower ingrowth of nucleogenic ^{21}Ne* compared to MORB, this requires a lower ^{3}He/^{22}Ne ratio in the respective mantle source, i.e. we need a process that depletes He relative to Ne. If the lithosphere simply represents degassed MORB, the higher solubility of He in silicate melts (e.g. Lux, 1987) would lead to a preferential enrichment of helium, i.e. the opposite of the required helium depletion relative to neon. Fluids/gases exsolved from a melt phase are expected to display low He/Ne ratios in course of solubility-controlled elemental fractionation. Hence, a strong metasomatic impregnation with e.g. water- or CO_2-rich fluids at the time of lithosphere stabilization is a potential process that could decrease the He/Ne ratio in the SCLM relative to MORB. So far, metasomatic enrichment processes of the East African lithospheric mantle at various times and scales remains speculative, but possible (e.g. Kalt et al., 1997).

Less nucleogenic ^{21}Ne/^{22}Ne ratios of a lithospheric mantle source are often attributed to addition of Loihi-type 'plume' noble gases (Buikin et al., 2005; Hopp et al., 2004; Matsumoto et al., 1997), that are mixed with a more nucleogenic lithospheric component (^{21}Ne/^{22}Ne ~ 0.07). To test a non-'plume' origin needs investigation of exposed sample locations, where 'plume' related activity is considered unlikely. Unfortunately our sample suites are biased. Cold unactive lithosphere will not supply us with mantle xenoliths and igneous rocks in general. However, during continental intraplate volcanism the initial trigger of this activity will influence our sample compositions. One way out could be investigations of peridotite massifs that had been tectonically emplaced and that are undoubtly not inside a sphere of influence of a known 'high ^{3}He/^{4}He' hotspot. There are only few studies on those massifs that unfortunately are not compelling enough for this purpose (Matsumoto et al., 2001, 2005). This is partly due to the high ages of many massifs leading to in situ radiogenic/nucleogenic contributions. Another problem is a severe contamination with crustal and/or atmospheric noble gases, blanketing any mantle signature. Thus, the existence of an intrinsic lithosphere composition with associated more radiogenic He and less nucleogenic Ne relative to MORB remains speculative. Therefore, it is justified to discuss below the presence

of a Loihi-type 'plume' neon component as a source of low $^{21}Ne/^{22}Ne$ ratios.

5.2. Evidence for a Kenyan 'plume' component?

The neon isotopic composition is the only compelling fingerprint of a mantle source composition that could directly be assigned to a Loihi-type 'plume' source. The extrapolated mantle $^{21}Ne/^{22}Ne$ ratios (for a mantle $^{20}Ne/^{22}Ne = 12.5$) of 0.050–0.056 are less nucleogenic than typical MORB composition (0.059–0.06), but still more nucleogenic than Loihi- or Iceland-type compositions (0.035–0.036, Trieloff et al., 2000; Valbracht et al., 1997). From the more radiogenic $^{3}He/^{4}He$ ratios (6–7 R_A) observed in this study compared with MORB (8±1 R_A, Graham, 2002) or 'high $^{3}He/^{4}He$' hotspots (up to 50 R_A, Stuart et al., 2003) we would expect a significant more nucleogenic Ne isotopic composition. This kind of isotope systematics in samples representing the subcontinental lithospheric mantle is now frequently found (Buikin et al., 2005; Hopp et al., 2004) and attributed by us to mixing between a 'plume' type component having a lower $^{3}He/^{22}Ne$ and an intrinsic lithospheric component with a higher $^{3}He/^{22}Ne$. Hence, the lithospheric component dominates the He isotope composition whereas Ne isotopes reflect a higher and detectable amount of 'plume' contributions. In Fig. 6 we plotted obtained mantle $^{21}Ne/^{22}Ne$ ratios against $^{4}He/^{3}He$ (black circles). All data fall in the same field as other examples of subcontinental lithospheric mantle (shown as light grey squares). Oceanic data (MORB, OIB) are shown as grey stars. The data distribution can be interpreted as binary mixing of an already evolved Loihi-type 'plume' component with an intrinsic lithospheric or asthenospheric (MORB-like) component. An initial radiogenic evolution with a constant $^{3}He/^{22}Ne$ (c. 7.7 assuming a common mantle production ratio of $^{4}He^*/^{21}Ne^* = 2.1 \cdot 10^7$, Yatsevich and Honda, 1997) for 'plume' and MORB, SCLM sources is represented in the linear trend. Before mixing, fractionation between He and Ne in one or both endmembers must have occurred. This could be accomplished e.g. by differences in element partitioning during partial melting. Subsequent mixing of both melt regimes via the melt phase then could produce observed isotope patterns. For the oceanic area this had already been proposed by Moreira and Allègre (1998). The resulting different $^{3}He/^{22}Ne$ ratios of admixed endmember compositions lead to hyperbolic mixing trajectories, with the r-values representing the $(^{3}He/^{22}Ne)_{MORB,\ SCLM}/(^{3}He/^{22}Ne)_{PLUME}$ ratio (Fig. 6). Two trends are shown for visualization: a mixing trend between 'plume' and MORB, and between 'plume' with

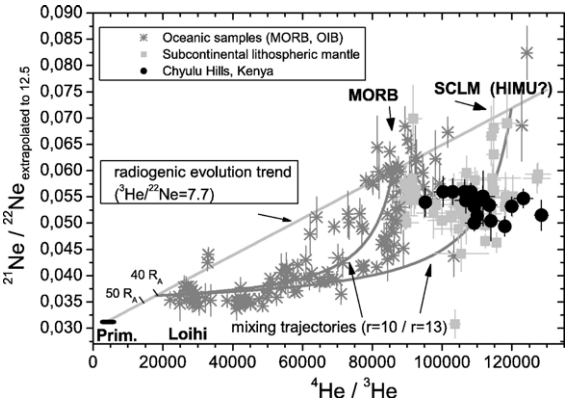

Fig. 6. $^{4}He/^{3}He$–$^{21}Ne/^{22}Ne$ isotope space, the latter corrected for atmospheric neon assuming a mantle $^{20}Ne/^{22}Ne = 12.5$. Data encompass oceanic settings (MORB, OIB), subcontinental lithosphere and results of this study (Barfod et al., 1999; Buikin et al., 2005; Hanyu et al., 2001; Hopp et al., 2004; Hopp and Trieloff, 2005; Kurz et al., 2005; Matsumoto et al., 1998; Moreira et al., 1995, 1996, 1998, 2001; Niedermann and Bach, 1998; Niedermann et al., 1997; Sarda et al., 1988, 2000; Staudacher et al., 1990; Trieloff et al., 2000, 2002; Valbracht et al., 1997). Uncertainties are 1σ. Only data with 1σ-uncertainties <10% are drawn. Details in Section 5.2.

a postulated more radiogenic/nucleogenic lithospheric endmember. The less nucleogenic neon isotope composition of the Kenyan xenoliths compared to MORB and postulated subcontinental lithospheric mantle compositions precludes a simple MORB–SCLM mixing scenario. From the data distribution in Fig. 6 a possible ternary mixing between MORB, 'plume' and lithospheric components appears more likely. The lithospheric component could be representative of an HIMU component that typically displays radiogenic $^{3}He/^{4}He$ ratios lower than MORB ratios (e.g. Hanyu and Kaneoka, 1997). Such an HIMU component, defined by very radiogenic $^{206}Pb/^{204}Pb$ ratios >20, is frequently found in volcanic rocks from the EAR system, but considering its Sr–Nd isotopic composition, it is certainly not identical with oceanic HIMU sources (Kalt et al., 1997).

The source of the 'plume' endmember still has to be identified. Because the Afar mantle 'plume' source must be considered as primitive (Marty et al., 1996; Scarsi and Craig, 1996), it would be the primary candidate for supplying volatiles to the southerly EAR system. Previous studies (Hopp et al., 2004; Moreira et al., 1996) demonstrated with He–Ne systematics the far reaching influence of the 'high ^{3}He' Afar hotspot even 2000–2500 km north of Afar. The distance to Chyulu Hills is similar (c. 2000 km), however, there is no mature oceanic ridge system inbetween both locations that indicates a large scale asthenospheric swell. This might be important in transport of noble gases – and fluids in

general – via melt percolation on regional scales. Therefore, we cannot discard a distinct Kenyan 'plume' component that would supply the necessary primordial noble gases. The supply rate must be low in comparison to Afar, in agreement with the less obvious geochemical 'plume' character of the east African rift related volcanics. There seems some minor difference in Pb–Sr–Nd isotope compositions of mafic volcanic rocks of the EAR system and of the Ethiopian flood basalt province (Macdonald et al., 2001; Pik et al., 2006; Rogers et al., 2000) that do also favour a separate Kenyan mantle 'plume' contribution. However, it remains an open question if these isotope systems are capable in tracing source signatures on a regional scale (>1000 km). Because of their volatility and, hence, mobility contributions of deep-seated 'plume' related noble gases might be broadly decoupled from other radiogenic isotope systems (Hopp et al., 2004). Therefore, we cannot discriminate a contribution of 'plume' related noble gases associated with the Afar mantle 'plume' source in Kenyan mantle rocks using Sr–Nd–Pb isotopes.

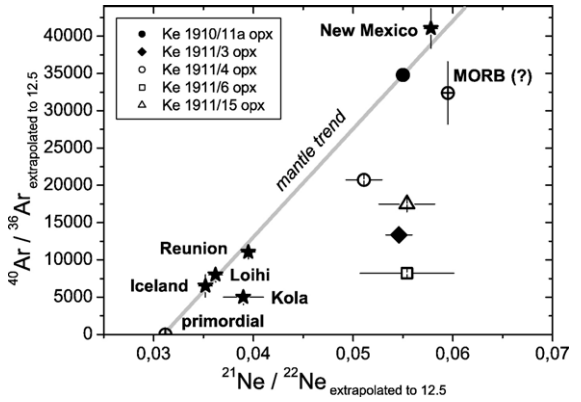

Fig. 7. Calculated mantle $^{40}Ar/^{36}Ar$ and $^{21}Ne/^{22}Ne$ ratios corrected for atmospheric contributions assuming a mantle $^{20}Ne/^{22}Ne = 12.5$. Estimates for other settings (Iceland, Loihi, Réunion, Kola, New Mexico well gas) are shown for comparison (Holland and Ballentine, 2006; Hopp and Trieloff, 2005; Marty et al., 1998; Trieloff and Kunz, 2005). Oceanic samples and continental samples with highest $^{40}Ar/^{36}Ar$ ratios seem to follow the same linear radiogenic evolution trend. Primordial values: $^{40}Ar/^{36}Ar \approx 0$ and $^{21}Ne/^{22}Ne = 0.03118$ (Trieloff and Kunz, 2005). Uncertainties are 1σ.

5.3. Ar and Xe compositions: some implications

In general, the Ar–Ne isotope systematics of the Kenyan SCLM is quite similar to systematics of the SCLM below the Red Sea region (Hopp et al., 2007). Hence, our interpretation is identical and we therefore only summarize shortly the most prominent conclusions, else referring to Hopp et al. (2007).

The $^{40}Ar/^{36}Ar$ source compositions of the mantle xenoliths appear highly variable, ranging from c. 8000 to 34 800. We find no correlation with mantle $^{21}Ne/^{22}Ne$ ratios (Fig. 7). However, the highest air corrected $^{40}Ar/^{36}Ar$ ratio (grt–orthopyroxenite Ke 1910/11a opx) agrees with the postulated mantle trend defined by us in previous studies (Hopp and Trieloff, 2005; Hopp et al., 2007). Complementary, the mantle $^{36}Ar/^{22}Ne$ ratios vary from values close to typical mantle ratios of about 10 towards higher ratios, indicating some sample specific Ar enrichment. Though, with few exceptions, $^{36}Ar/^{22}Ne$ ratios are not well constrained, a correlated behaviour with $^{40}Ar/^{36}Ar$ seems to exist: In a diagram of $^{40}Ar/^{36}Ar$ ratios versus $^{22}Ne/^{36}Ar$ ratios (supplementary Fig. 4) a linear correlation can be constructed, that passes the origin and points to the addition of a ^{36}Ar-rich contaminant (relative to neon). Because the values with low $^{22}Ne/^{36}Ar$ have high uncertainties the correlation is preliminary and needs further data support.

We can expand our mixing hypothesis in the He–Ne isotope space to the Ar–Ne isotope space. We may reasonably assume that the 'plume' component is characterized by a lower $^{40}Ar/^{36}Ar$ ratio than the SCLM or MORB components. The observed variation of $^{40}Ar/^{36}Ar$ ratios relative to air corrected $^{21}Ne/^{22}Ne$ values (Fig. 7) would necessitate a strongly curved hyperbolic mixing trend between this 'plume' and the respective lithospheric or asthenospheric endmember composition. This requires a 'plume' component with an elevated $^{36}Ar/^{22}Ne$ ratio relative to the lithospheric/asthenospheric mantle sources, in agreement with a sequence of fractionation in favour of the heavier element within the mantle 'plume' source. But in contrast to the He–Ne isotope space (Fig. 6) we cannot trace a hyperbolic relationship between air corrected $^{40}Ar/^{36}Ar$ and $^{21}Ne/^{22}Ne$ ratios (Fig. 7) in mantle rocks as direct evidence for mixing and fractionation.

Alternatively, an apparent ^{36}Ar-enrichment of the lithospheric mantle source leading to elevated $^{36}Ar/^{22}Ne$ and lowered $^{40}Ar/^{36}Ar$ ratios could reflect addition of an elementally fractionated atmospheric component with high $^{36}Ar/^{22}Ne$ ratios. As we shortly addressed in the 'results'-section, water (groundwater, seawater, meteoric water) is enriched in Ar relative to Ne (e.g. Ballentine et al., 2002). The source of this atmospheric component might be shallow, e.g. addition of atmospheric fluids into the host magma at shallow depth and mixing of these fluids with the mantle fluids derived from larger depth. However, we also can imagine a subduction related origin of this atmospheric

component. From analyses of New Mexican well-gases Holland and Ballentine (2006) deduced that a significant amount of seawater derived atmospheric heavy noble gases (Ar, Kr, Xe) is present in the local mantle source and proposed a subduction related origin. It was shown, that for the Red Sea lithospheric mantle a subduction related transfer of atmospheric noble gases, enriched in Ar relative to Ne, could account for the observed variation in $^{40}Ar/^{36}Ar$ ratios in spite of the high age of the last subduction event during the Pan-African orogeny (c. 700 Ma) (Hopp et al., 2007). The youngest ages of the Pan-African orogeny at Kenya are even younger (about 550 Ma). A possible subduction related addition of Xe would also agree with observed $^{132}Xe/^{36}Ar$ and $^{132}Xe/^{22}Ne$ ratios, that are similarly elevated as the $^{36}Ar/^{22}Ne$ ratios. However, we have no information regarding the $^{132}Xe/^{36}Ar$, $^{132}Xe/^{22}Ne$ elemental ratios and Xe isotope ratios of the mantle source. Hence, we cannot distinguish between a deep (= slab derived) or shallow origin of the observed fractionated, Ar- and Xe-rich atmospheric components.

6. Summary and conclusions

The Ne isotopic composition in mantle xenoliths from the Chyulu Hills volcanic field, S Kenya, agrees with a contribution of a primitive mantle 'plume' source in the trapped fluids., We are, however, not able to distinguish whether this source is equivalent to the long postulated Kenyan mantle 'plume' or if our results point to the southern border of influence of the Afar hotspot c. 2000 km to the north. Alternatively, the widespread observation of similar neon isotope characteristics in samples from SCLM could point to a distinct lithospheric signature.

In contrast to neon isotopes, $^{3}He/^{4}He$ ratios are 6–7 R_A, i.e. lower than average MORB values and thus in the typical range for subcontinental lithospheric mantle worldwide. There is no evidence for helium contributions of a 'high $^{3}He/^{4}He$' hotspot.

Air corrected mantle $^{40}Ar/^{36}Ar$ ratios are variable and encompass values of 8000 to 34 800. A similar variability was previously observed at other locations and might be attributed to a cryptic addition of a highly elementally fractionated atmospheric component or mixing between elementally fractionated mantle components (Buikin et al., 2005; Hopp et al., 2007). The maximum calculated $^{40}Ar/^{36}Ar$ ratio for one garnet orthopyroxenite is in accordance with common mantle evolution scenarios in Ar–Ne space. Thus, the trapped fluids appear to be uncontaminated or not affected by fractionation processes.

Xe isotopic compositions reveal the same correlated excess in ^{129}Xe and ^{136}Xe typically observed in mantle samples. The maximum $^{129}Xe/^{130}Xe$ and $^{136}Xe/^{130}Xe$ ratios are 7.01 ± 0.12 and 2.37 ± 0.05, respectively, and thus intermediate in comparison to reported maximum ratios in MORB and OIB samples (Hopp and Trieloff, 2005; Moreira et al., 1998; Kunz et al., 1998; Poreda and Farley, 1992; Trieloff et al., 2000, 2002). This nicely coincides with Ne isotopes, however, these Xe ratios only can serve as lower limits for the respective source composition.

Acknowledgements

We like to thank Sandra Panienka for her patient and careful high quality handpicking of the mineral separates. E. Burkert, W. Hampel, J. Kiko and G. Zuzel at the Max-Planck-Institut for nuclear physics continuously supported this work. Helpful comments by D. Hilton and C. Ballentine considerably improved our manuscript. JH acknowledges funding from Deutsche Forschungsgemeinschaft, grant HO 2591/1-1 and HO 2591/2-1.

Appendix A. Supplementary data

Supplementary data associated with this article can be found, in the online version, at doi:10.1016/j.epsl.2007.07.027.

References

Altherr, R., Garasic, V., Ulianov, A., Kalt, A., in revision. Mantle xenoliths from the Chyulu Hills Volcanic Province (Kenya, East African Rift system): Constraints on lithospheric evolution and magma genesis. J. Petrol. in revision.

Baker, B.H., 1987. Outline of the petrology of the Kenya rift alkaline province. In: Fitton, J.G., Upton, B.G.J. (Eds.), Alkaline Igneous Rocks. Geol. Soc. London Sp. Publ., 30, pp. 293–311.

Ballentine, C.J., Burgess, R., Marty, B., 2002. Tracing fluid origin, transport and interaction in the crust. In: Porcelli, D.R., Ballentine, C.J., Wieler, R. (Eds.), Noble Gases in Geochemistry and Cosmochemistry. Reviews in Mineralogy and Geochemistry, vol. 47, pp. 539–614.

Ballentine, C.J., Marty, B., Sherwood Lollar, B., Cassidy, M., 2005. Neon isotopes constrain convection and volatile origin in the Earth's mantle. Nature 433, 33–38.

Barfod, D.N., Ballentine, C.J., Halliday, A.N., Fitton, J.G., 1999. Noble gases in the Cameroon line and the He, Ne, and Ar isotopic compositions of high μ (HIMU) mantle. J. Geophys. Res. 104, 29509–29527.

Bell, K., Tilton, G.R., 2001. Nd, Pb and Sr isotopic compositions of East African carbonatites: evidence for mantle mixing and plume inhomogeneity. J. Petrol. 42, 1927–1945.

Benoit, M.H., Nyblade, A.A., VanDecar, J.C., 2006. Upper mantle P-wave speed variations beneath Ethiopia and the origin of the Afar hotspot. Geology 34, 329–332.

Buikin, A.I., Trieloff, M., Hopp, J., Althaus, T., Korochantseva, E.V., Schwarz, W.H., Altherr, R., 2005. Noble gas isotopes suggest deep mantle plume source of late Cenozoic mafic alkaline volcanism in Europe. Earth Planet. Sci. Lett. 230, 143–162.

Clarke, W.B., Beg, M.A., Craig, H., 1969. Excess ^{3}He in the sea: evidence for terrestrial primordial helium. Earth Planet. Sci. Lett. 6, 213–220.

Darling, W.G., Griesshaber, E., Andrews, J.N., Armannsson, H., O'Nions, R.K., 1995. The origin of hydrothermal and other gases in the Kenyan Rift Valley. Geochim. Cosmochim. Acta 59, 2501–2512.

Day, J.M.D., Hilton, D.R., Pearson, D.G., Macpherson, C.G., Kjarsgaard, B.A., Janney, P.E., 2005. Absence of a high time-integrated ^{3}He/(U+Th) source in the mantle beneath continents. Geology 33, 733–736.

Debayle, E., Lévêque, J.-J., Cara, M., 2001. Seismic evidence for a deeply rooted low-velocity anomaly in the upper mantle beneath the northeastern Afro/Arabian continent. Earth Planet. Sci. Lett. 193, 423–436.

Drescher, J., Kirsten, T., Schäfer, K., 1998. The rare gas inventory of the continental crust, recovered by the KTB Continental Deep Drilling Project. Earth Planet. Sci. Lett. 154, 247–263.

Dunai, T.J., Porcelli, D.R., 2002. Storage and transport of noble gases in the subcontinental lithosphere. In: Porcelli, D.R., Ballentine, C.J., Wieler, R. (Eds.), Noble Gases in Geochemistry and Cosmochemistry. Reviews in Mineralogy and Geochemistry, vol. 47, pp. 237–249.

Ebinger, C.J., Bechel, T.D., Forsyth, D.W., Bowin, C.O., 1989. Effective elastic thickness beneath the East African and Afar plateaus and dynamic compensation of uplift. J. Geophys. Res. 94, 2883–2901.

Ebinger, C.J., Sleep, N.H., 1998. Cenozoic magmatism throughout East Africa resulting from impact of a single plume. Nature 395, 788–791.

Furman, T., Graham, D., 1999. Erosion of lithospheric mantle beneath the East African Rift system: geochemical evidence from the Kivu volcanic province. Lithos 48, 237–262.

Furman, T., Kaleta, K.M., Bryce, J.G., Hanan, B.B., 2006. Tertiary mafic lavas of Turkana, Kenya: constraints on East African plume structure and the occurrence of high-μ volcanism in Africa. J. Petrol. 47, 1221–1244.

Gautheron, C., Moreira, M., 2002. Helium signature of the subcontinental lithospheric mantle. Earth Planet. Sci. Lett. 199, 39–47.

Graham, D.W., Noble gas isotope geochemistry of Mid-Ocean ridge and Ocean Island basalts: Characterization of mantle source reservoirs, in: Porcelli, D.R., Ballentine, C.J., Wieler, R. (Eds.), Noble gases in geochemistry and cosmochemistry. Reviews in Mineralogy and Geochemistry, vol. 47, pp. 247–318.

Hanyu, T., Kaneoka, I., 1997. The uniform and low ^{3}He/^{4}He ratios of HIMU basalts as evidence for their origin as recycled materials. Nature 390, 273–276.

Hanyu, T., Dunai, T.J., Davies, G.R., Kaneoka, I., Nohda, S., Uto, K., 2001. Noble gas study of the Réunion hotspot: evidence for distinct less-degassed mantle sources. Earth Planet. Sci. Lett. 193, 83–98.

Haug, G.H., Strecker, M.R., 1995. Volcano-tectonic evolution of the Chyulu Hills and implications for the regional stress field in Kenya. Geol. 23, 165–168.

Henjes-Kunst, F., Altherr, R., 1992. Metamorphic petrology of xenoliths from Kenya and northern Tanzania and implications for geotherms and lithospheric structures. J. Petrol. 33, 1125–1156.

Hilton, D.R., Gronvold, K., Sveinbjornsdottir, A.E., Hammerschmidt, K., 1998. Helium isotope evidence for off-axis degassing of the Icelandic hotspot. Chem. Geol. 149, 173–187.

Hiyagon, H., Ozima, M., Marty, B., Zashu, S., Sakai, H., 1992. Noble gases in submarine glasses from mid-ocean ridges and Loihi seamount: constraints on the early history of the Earth. Geochim. Cosmochim. Acta 56, 1301–1316.

Holland, G., Ballentine, C.J., 2006. Seawater subduction controls the heavy noble gas composition of the mantle. Nature 441, 186–191.

Honda, M., McDougall, I., Patterson, D.B., Doulgeris, A., Clague, D.A., 1991. Possible solar noble-gas component in Hawaiian basalts. Nature 349, 149–151.

Hopp, J., Trieloff, M., Altherr, R., 2004. Ne isotopes in mantle rocks from the Red Sea region reveal large scale plume–lithosphere interaction. Earth Planet. Sci. Lett. 219, 61–76.

Hopp, J., Trieloff, M., 2005. Refining the noble gas record of the Réunion mantle plume source: implications on mantle geochemistry. Earth Planet. Sci. Lett. 240, 573–588.

Hopp, J., Trieloff, M., Buikin, A.I., Korochantseva, E.V., Schwarz, W.H., Althaus, T., Altherr, R., 2007. Heterogeneous mantle argon isotope composition in the subcontinental lithospheric mantle beneath the Red Sea region. Chem. Geol. 240, 36–53.

Kalt, A., Hegner, E., Satir, M., 1997. Nd, Sr, and Pb isotopic evidence for diverse lithospheric mantle sources of East African Rift carbonatites. Tectonophysics 278, 31–45.

Kunz, J., Staudacher, T., Allègre, C.J., 1998. Plutonium-fission xenon found in Earth's mantle. Science 280, 877–880.

Kurz, M.D., Moreira, M., Curtice, J., Lott III, D.E., Mahoney, J.J., Sinton, J.M., 2005. Correlated helium, neon, and melt production on the super-fast spreading East Pacific Rise near 17°S. Earth Planet. Sci. Lett. 232, 125–142.

Lux, G., 1987. The behaviour of noble gases in silicate liquids: solution, diffusion, bubbles and surface effects, with applications to natural samples. Geochim. Cosmochim. Acta 51, 1549–1560.

Macdonald, R., Rogers, N.W., Fitton, J.G., Black, S., Smith, M., 2001. Plume–lithosphere interactions in the generation of the basalts of the Kenya Rift, East Africa. J. Petrol. 42, 877–900.

Marty, B., 1989. Neon and xenon isotopes in MORB: implications for the earth–atmosphere evolution. Earth Planet. Sci. Lett. 94, 45–56.

Marty, B., Pik, R., Gezahegn, Y., 1996. Helium isotopic variations in Ethiopian plume lavas: nature of magmatic sources and limit on lower mantle contribution. Earth Planet. Sci. Lett. 144, 223–237.

Marty, B., Tolstikhin, I., Kamensky, I.L., Nivin, V., Balaganskaya, E., Zimmermann, J.-L., 1998. Plume-derived rare gases in 380 Ma carbonatites from the Kola region (Russia) and the argon isotopic composition in the deep mantle. Earth Planet. Sci. Lett. 164, 179–192.

Matsumoto, T., Honda, M., McDougall, I., Yatsevich, I., O'Reilly, S.Y., 1997. Plume-like neon in a metasomatic apatite from the Australian lithospheric mantle. Nature 388, 162–164.

Matsumoto, T., Honda, M., McDougall, I., O'Reilly, S.Y., 1998. Noble gases in anhydrous lherzolites from the Newer Volcanics, southeastern Australia: a MORB-like reservoir in the subcontinental mantle. Geochim. Cosmochim. Acta 62, 2521–2533.

Matsumoto, T., Honda, M., McDougall, I., O'Reilly, S.Y., Norman, M., Yaxley, G., 2000. Noble gases in pyroxenites and metasomatised peridotites from the Newer Volcanics, southeastern Australia: implications for mantle metasomatism. Chem. Geol. 168, 49–73.

Matsumoto, T., Chen, Y., Matsuda, J., 2001. Concomitant occurence of primordial and recycled noble gases in the Earth's mantle. Earth Planet. Sci. Lett. 185, 35–47.

Matsumoto, T., Morishita, T., Matsuda, J., Fujioka, T., Takebe, M., Yamamoto, K., Arai, S., 2005. Noble gases in the Finero phlogopite–peridotites, western Italian Alps. Earth Planet. Sci. Lett. 238, 130–145.

McDougall, I., Watkins, R.T., 1988. Potassium–argon ages of volcanic rocks from the northeast of Lake Turkana, northern Kenya. Geol. Mag. 125, 15–23.

Moreira, M., Staudacher, T., Sarda, P., Schilling, J.G., Allègre, C.J., 1995. A primitive plume neon component in MORB: the Shona ridge-anomaly, South Atlantic (51–52°S). Earth Planet. Sci. Lett. 133, 367–377.

Moreira, M., Valbracht, P.J., Staudacher, T., Allègre, C.J., 1996. Rare gas systematics in Red Sea ridge basalts. Geophys. Res. Lett. 23, 2453–2456.

Moreira, M., Allègre, C.J., 1998. Helium–neon systematics and the structure of the mantle. Chem. Geol. 147, 53–59.

Moreira, M., Kunz, J., Allègre, C.J., 1998. Rare gas systematics in Popping Rock: isotopic and elemental compositions in the upper mantle. Science 279, 1178–1181.

Moreira, M., Breddam, K., Curtice, J., Kurz, M.D., 2001. Solar neon in the Icelandic mantle: new evidence for an undegassed lower mantle. Earth Planet. Sci. Lett. 185, 15–23.

Morley, C.K., 1999. Tectonic evolution of the East African Rift system and the modifying influence of magmatism: a review. Acta Vulcanol. 11, 1–19.

Niedermann, S., Bach, W., Erzinger, J., 1997. Noble gas evidence for a lower mantle component in MORBs from the southern East Pacific Rise: decoupling of helium and neon isotope systematics. Geochim. Cosmochim. Acta 61, 2697–2715.

Niedermann, S., Bach, W., 1998. Anomalously nucleogenic neon in North Chile Ridge basalt glasses suggesting a previously degassed mantle source. Earth Planet. Sci. Lett. 160, 447–462.

Novak, O., Ritter, J.R.R., Altherr, R., Garasic, V., Volker, F., Kluge, C., Kaspar, T., Byrne, G.F., Sobolev, S.V., Fuchs, K., 1997. An integrated model for the deep structure of the Chyulu Hills volcanic field, Kenya. Tectonophysics 287, 187–209.

Nyblade, A.A., Owens, T.J., Gurrola, H., Ritsema, J., Langston, C.A., 2000. Seismic evidence for a deep upper mantle thermal anomaly beneath East Africa. Geology 28, 599–602.

Ozima, M., Podosek, F.A., 2002. Noble Gas Geochemistry, 2nd ed. Cambridge University press, Cambridge.

Pik, R., Deniel, C., Coulon, C., Yirgu, G., Marty, B., 1999. Isotopic and trace element signatures of Ethiopian flood basalts: evidence for plume–lithosphere interactions. Geochim. Cosmochim. Acta 63, 2263–2279.

Pik, R., Marty, B., Hilton, D.R., 2006. How many mantle plumes in Africa? The geochemical point of view. Chem. Geol. 226, 100–114.

Poreda, R.J., Farley, K.A., 1992. Rare gases in Samoan xenoliths. Earth Planet. Sci. Lett. 113, 129–144.

Rogers, N., Macdonald, R., Fitton, J.G., George, R., Smith, M., Barreiro, B., 2000. Two mantle plumes beneath the East African rift system: Sr, Nd and Pb isotope evidence from Kenya Rift basalts. Earth Planet. Sci. Lett. 176, 387–400.

Rogers, N.W., Thomas, L.E., Macdonald, R., Hawkesworth, C.J., Mokadem, F., 2006. ^{238}U–^{230}Th disequilibrium in recent basalts and dynamic melting beneath the Kenya rift. Chem. Geol. 234, 148–168.

Sarda, P., Staudacher, T., Allègre, C.J., 1988. Neon isotopes in submarine basalts. Earth Planet. Sci. Lett. 91, 73–88.

Sarda, P., Moreira, M., Staudacher, T., 2000. Rare gas systematics on the southernmost Mid-Atlantic Ridge: constraints on the lower mantle and the Dupal source. J. Geophys. Res. 105, 5973–5996.

Scarsi, P., Craig, H., 1996. Helium isotope ratios in Ethiopian Rift basalts. Earth Planet. Sci. Lett. 144, 505–516.

Scarsi, P., 2000. Fractional extraction of helium by crushing of olivine and clinopyroxene phenocrysts: effects on the $^{3}He/^{4}He$ measured ratio. Geochim. Cosmochim. Acta 64, 3751–3762.

Sebai, A., Stutzmann, E., Montagner, J.-P., Sicilia, D., Beucler, E., 2006. Anisotropic structure of the African upper mantle from Rayleigh and Love wave tomography. Phys. Earth Planet. Inter. 155, 48–62.

Späth, A., Le Roex, A.P., Opiyo-Akech, N., 2001. Plume–lithosphere interaction and the origin of continental rift-related alkaline volcanism — the Chyulu Hills Volcanic Province, southern Kenya. J. Petrol. 42, 765–787.

Staudacher, T., Allègre, C.J., 1982. Terrestrial xenology. Earth Planet. Sci. Lett. 60, 389–406.

Staudacher, T., Sarda, P., Allègre, C.J., 1990. Noble gas systematics of Réunion Island, Indian Ocean. Chem. Geol. 89, 1–17.

Stuart, F.M., Lass-Evans, S., Fitton, J.G., Ellam, R.M., 2003. High $^{3}He/^{4}He$ ratios in picritic basalts from Baffin Island and the role of a mixed reservoir in mantle plumes. Nature 424, 57–59.

Trieloff, M., Kunz, J., Clague, D.A., Harrison, D., Allègre, C.J., 2000. The nature of pristine noble gases in mantle plumes. Science 288, 1036–1038.

Trieloff, M., Kunz, J., Allègre, C.J., 2002. Noble gas systematics of the Réunion mantle plume source and the origin of primordial noble gases in Earth's mantle. Earth Planet. Sci. Lett. 200, 297–313.

Trieloff, M., Kunz, J., 2005. Isotope systematics of noble gases in the Earth's mantle: possible sources of primordial isotopes and implications for mantle structure. Phys. Earth Planet. Inter. 148, 13–38.

Ukstins, I.A., Renne, P.R., Wolfenden, E., Baker, J., Ayalew, D., Menzies, M., 2002. Matching conjugate volcanic rifted margins: $^{40}Ar/^{39}Ar$ chrono-stratigraphy of pre- and syn-rift bimodal flood volcanism in Ethiopia and Yemen. Earth Planet. Sci. Lett. 198, 289–306.

Ulianov, A., Kalt, A., Pettke, T., 2006. Peraluminous websterite and granulite xenoliths from the Chyulu Hills volcanic field, Kenya: plagioclase-bearing cumulates reequilibrated at uppermost mantle and crustal conditions. Contrib. Mineral. Petrol. 152, 459–483.

Valbracht, P.J., Staudacher, T., Malahoff, A., Allègre, C.J., 1997. Noble gas systematics of deep rift zone glasses from Loihi Seamount, Hawaii. Earth Planet. Sci. Lett. 150, 399–411.

Weeraratne, D.S., Forsyth, D.W., Fischer, K.M., Nyblade, A.A., 2003. Evidence for an upper mantle plume beneath the Tanzanian craton from Rayleigh wave tomography. J. Geophys. Res. 108, 2427–2434.

Yatsevich, I., Honda, M., 1997. Production of nucleogenic neon in the Earth from natural radioactive decay. J. Geophys. Res. 102, 10291–10298.

Yokochi, R., Marty, B., 2005. Geochemical constraints on mantle dynamics in the Hadean. Earth Planet. Sci. Lett. 238, 17–30.

Zindler, A., Hart, S., 1986. Chemical geodynamics. Ann. Rev. Earth Planet. Sci. 14, 493–571.